# A Novel *Porphyromonas gingivalis* Infection-Related Inflammatory Response-Related Genes Signature Predicts the Prognosis of Esophageal Squamous Cell Carcinoma

Jinyu Kong[1,2] ID, Yiwen Liu[2], Jian Wang[3], Mengfan Qian[2], Wei Sun[2] and Ling Xing[1]

[1]School of Information Engineering, Henan University of Science and Technology, Luoyang, China.
[2]Cancer Hospital, The First Affiliated Hospital and College of Clinical Medicine, Henan University of Science and Technology, Luoyang, China. [3]Center of Image Diagnoses, The First Affiliated Hospital and College of Clinical Medicine, Henan University of Science and Technology, Luoyang, China.

## ABSTRACT

**BACKGROUND:** Our previous research showed that *Porphyromonas gingivalis* (*P. gingivalis*) infection can activate the inflammatory signaling pathway and promotes the malignancy development of esophageal squamous cell carcinoma (ESCC). However, the prognostic significance of inflammatory response-related genes (IRRGs) in *P. gingivalis*-infected ESCC requires further elucidation. Hence, our study constructed a prognostic signature based on *P. gingivalis* and IRRGs to forecast the survival of patients with ESCC, which may provide insight into new treatment options for ESCC patients.

**METHODS:** Differentially expressed genes (DEGs) were identified in *P.gingivalis*-infected and *P.gingivalis*-uninfected ESCC cell by RNA sequencing. A risk model was constructed and validated using the The Cancer Genome Atlas (TCGA) and Gene Expression Omnibus (GEO) database by using univariate Cox regression analysis, LASSO, and the multivariate Cox regression analysis. Kaplan-Meier analysis was carried out to compare the overall survival (OS) between high-risk and low-risk groups. Single-sample gene set enrichment analysis was used to analyze the immune cell infiltration. The Genomics of Drug Sensitivity in Cancer database was used to predict drug sensitivity.

**RESULTS:** There were 365 DEGs between the *P.gingivalis*-infected and *P.gingivalis*-uninfected groups. Four genes including DKK1, ESRRB, EREG, and RELN were identified to construct the prognostic risk model ($P = .012$, C-index = 0.73). In both the training and validation sets, patients had a considerably shorter OS in the high-risk group than those in the low-risk group ($P < .05$). A nomogram was established using the risk score, gender, and N stage which could effectively forecast the prognosis of patients ($P = .016$, C-index = 0.66). The high-risk group displayed lower immune infiltrating cells, such as activated dendritic cells, type 2 T helper cells, and neutrophils ($P < .05$). A total of 41 drugs, including dactinomycin, luminespib, and sepantronium bromide, had a significant difference in IC50 between the 2 subgroups.

**CONCLUSION:** We demonstrated the potential of a novel signature constructed from 4 *P. gingivalis*-related IRRGs for prognostic prediction in ESCC patients.

**KEYWORDS:** Esophageal squamous cell carcinoma, inflammatory response, *Porphyromonas gingivalis*, prognosis, immune microenvironment, signature

## Introduction

Esophageal cancer (EC) is a malignant tumor that has a significant incidence and fatality rate. In 2020, there were 604 100 new cases and 544 076 deaths of EC worldwide.[1] This ranks EC as the seventh most common cancer by incidence and the sixth deadliest malignancy. China, in particular, bears a high burden of EC, with more than 90% of cases being esophageal squamous cell carcinoma (ESCC).[2] In 2020, China reported 324 000 new cases and 301 000 deaths from EC, accounting for ~55% of the global figures.[1,3] Despite advancements in multimodal therapies such as surgical procedures, chemotherapy, radiotherapy, and targeted therapy, the overall 5-year survival rate for EC is still less than 20%.[4] Hence, it is crucial to identify novel prognostic signatures to assess individualized survival risk for patients with ESCC.

Mounting evidence suggests that the microbiome of the esophagus, along with inflammation and their interaction, play a crucial role in promoting EC.[5] It is estimated that 25% of all malignant tumor cases worldwide can be attributed to long-term infection and inflammation.[6] *Porphyromonas gingivalis* (*P. gingivalis*), a significant pathogenic bacterium associated with local immune inflammatory responses in long-term periodontitis, has garnered attention in recent years due to its close association with various malignant tumors.[7,8] *Porphyromonas*

*gingivalis* has been found to be closely related to ESCC in recent years. In 2016, a study reported found that the infection rate of *P. gingivalis* in ESCC tissues (61%, 71%) were significantly higher than adjacent normal tissue (12%, 12%) and normalesophagealmucosaltissue(0%,1%)byimmunohistochemistry (IHC) and polymerase chain reaction (PCR). In addition, the mean survival time of *P. gingivalis*-positive patients was significantly lower than that of negative patients.[9] Another study discovered that serum *P. gingivalis* IgG and IgA antibody levels in ESCC patients were significantly higher than those in esophagitis patients and healthy control group (*P* < .01). And high levels of *P. gingivalis* IgG or IgA antibodies are associated with poor prognosis in ESCC patients.[10] Besides, there is enrichment of *P. gingivalis* in high-grade dysplasia and early ESCC, and overabundance of *P. gingivalis* was positively associated with invasion depth, postendoscopic submucosal dissection stricture and local recurrence.[11] Notably, patients with ESCC who were infected with *P. gingivalis* had poor chemotherapy responses and a significantly shortened 5-year survival rate following surgical intervention.[12,13] In conclusion, the above researches showed that *P. gingivalis* had a significant influence on the development and progression of ESCC, as well as its impact on the patient prognosis. Long-term inflammation is a key player in oncogenesis and tumor progression. Long-term inflammation induced by microbial infection significantly elevates the possibility of carcinogenesis by way of activating inflammatory signaling pathways and cytokines, stimulating cell proliferation, and inhibiting apoptosis.[14] There is clear evidence that long-term colonization of *Helicobacter pylori*, *human papillomavirus*, and *hepatitis B virus* can accelerate the progression of stomach carcinoma, cervical carcinoma, and hepatocellular carcinoma by inducing long-term inflammation.[15] Wang et al[16] indicated that nuclear factor (NF)-kappa BP65 promotes invasion and metastasis of ESCC by regulating MMP9 and epithelial-mesenchymal transition (EMT). Besides, up-regulation of interleukin (IL)-6/STAT3 signaling pathway promotes the occurrence of EC.[17] Interleukin-6 is a cytokine that binds to gp130 through its receptor IL-6Rα, triggering the downstream pathway to activate important molecules such as SHP2, Ras-MAPK, STAT1, and STAT3.[18] These pathways activate the ability of tumor cells to survive in the inflammatory environment and inhibit the effects of immunotherapy. Interleukin-6 can drive the proliferation of myeloid-derived suppressor cells (MDSCs), and the activation of STAT3 leads to the production of antiapoptotic molecules, thus causing tumorigenesis.[19] *P. gingivalis* has been proven to induce inflammation and promote the malignant progression of ESCC by activating STAT3, GSK3β, NF-κβ, and tumor growth factor (TGF)-β signaling pathways.[8,20] In addition, the intratumoral *P. gingivalis* promotes the progression of pancreatic cancer by enhancing the secretion of neutrophilic chemokines and neutrophil elastase.[21] The fibrinogen/albumin ratio, neutrophil/lymphocyte ratio, and platelet/lymphocyte ratio, as markers of inflammation in circulating blood, have been shown to be associated with the prognosis of EC.[22,23] Previous studies have reported models based on inflammatory responses for prognostic predictions in EC.[24] This finding suggested that inflammation has an impact on cancer prognosis and can serve as a promising therapeutic target. However, the role and prognostic significance of inflammatory response-related genes (IRRGs) in *P. gingivalis*-infected ESCC remain unclear.

We first constructed an IRRG prognostic signature by using The Cancer Genome Atlas (TCGA)-ESCC data set and the RNA-seq data of *P. gingivalis*-infected ESCC cells in this study. Then we validated its prognostic value using the GSE53622 data set. Thereafter, a nomogram was constructed to predict the survival of patients with ESCC. Simultaneously, we explored the relationship between IRRGs and immune function, genetic mutation analysis, immunotherapy, and drug susceptibility. Our findings have the potential to improve comprehension of the prognostic mechanisms and provide novel and valuable biomarkers for treating patients of ESCC. The flowchart of this study is exhibited in Figure 1.

## Materials and Methods
### Cell culture, bacteria strain, and cell infection

The ESCC cell line Kyse-140 (BNCC351870, BeNa Culture Collection, China) was cultured at 37°C with 5% $CO_2$ in RPMI-1640 medium (PM150110, Procell, China) supplemented with 10% fetal bovine serum (164210-500, Procell, China). *P. gingivalis* ATCC 33277 was donated by the University of Louisville and was cultured at 37°C under anaerobic conditions consisting of 85% $N_2$, 10% $H_2$, and 5% $CO_2$ in Brain Heart Infusion (BHI) broth medium (237500, Becton Dickinson, USA) containing 0.1% Hemin and 0.1% Vitmin K1. The optical density of bacterial solution was measured at 600 nm by spectrophotometer with a value of 1.0 corresponding to $1 \times 10^9$ CFU/ml. Then centrifuge the bacterial solution at 12 000 g for 5 minutes, and remove the supernatant. Resuspend the *P. gingivalis* bacterial precipitate in 1 ml phosphate-buffered saline (PBS) and add it to Kyse-140 cell culture medium. Finally, cells were inoculated with *P. gingivalis* at a multiplicity of infection (MOI) of 20 for 24 hours at 37°C in 5% $CO_2$.

### Data sources

In this study, we performed transcriptome sequencing of Kyse-140 cells between *P. gingivalis*-infected and *P. gingivalis*-uninfected in the GENEWIZ Biotechnology Corporation. The TCGA-ESCC data set containing 80 tumor specimens and 11 normal specimens with clinical information and survival information (Table 1) available was sourced from the TCGA database (https://www.cancer.gov/ccg/). Moreover, we used the GSE53622 data set was achieved from the Gene Expression Omnibus (GEO) database (http://www.ncbi.nlm.nih.gov/
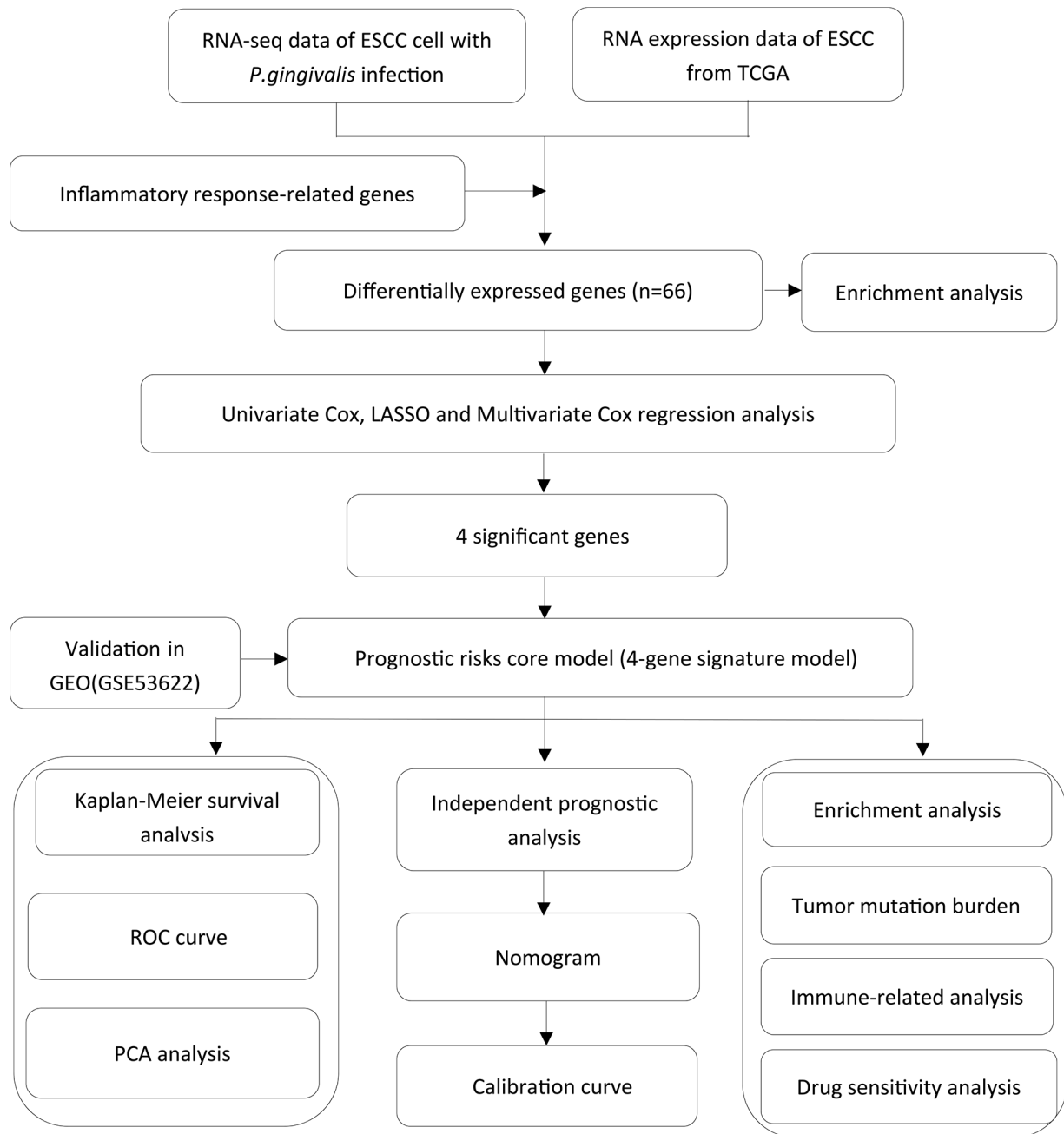
**Figure 1.** Flowchart of the present study.

geo/), containing 60 tumor samples and 60 control samples, as an external validation data set (Table 1). In addition, 3074 IRRGs were gathered from the GeneCards online database according to a score threshold >5. Furthermore, the IMvigor210 data set containing 298 cohort data of immunotherapy for bladder urothelial carcinoma (BLCA) was obtained from the IMvigor210 database.

### Acquisition analysis and enrichment analysis of crossover genes

Differentially expressed genes (DEGs) between the *P. gingivalis*-infected and *P. gingivalis*-uninfected group were identified using the DESeq2 (v1.36.0) R package ($P < .05$).[25]

Moreover, DEGs between ESCC and normal samples in the TCGA-ESCC data set were identified by the same method. To visualize the DEGs, we generated heat maps and volcano maps for the *P. gingivalis*-infected versus *P. gingivalis*-uninfected groups, and tumor versus normal groups were plotted by the heatmap (v0.7.7) and ggplot2 (v3.3.0) R packages, respectively.[26] Furthermore, we performed an intersection analysis to identify genes that were common between the DEGs in the self-sequencing data, DEGs in the TCGA-ESCC data set, and the set of IRRGs. In addition, to acquire understanding of the biological functions and signaling pathways associated with these crossover genes, we performed gene ontology (GO) functional enrichment analysis using the clusterProfiler (v3.8.1) R package with a significance threshold of $P < .05$.[27]

**Table 1.** Clinicopathological characteristics of ESCC patients in TCGA and GEO cohort.

| VARIABLES | TCGA-ESCC | GSE53622 |
|---|---|---|
| Tumor sample | 80 | 60 |
| Normal sample | 11 | 60 |
| Age (median, range) | 57 (36-90) | 60 (39-81) |
| Gender | | |
| Male | 69 (86.3%) | 48 (80%) |
| Female | 11 (13.7%) | 12 (20%) |
| Stage | | |
| I | 6 (7.5%) | 4 (6.7%) |
| II | 47 (58.8%) | 30 (50.0%) |
| III | 22 (27.5%) | 26 (43.3%) |
| IV | 3 (3.7%) | 0 |
| Unknown | 2 (2.5%) | |
| Survival status | | |
| Alive | 55 (68.7%) | 27 (45.0%) |
| Dead | 25 (31.3%) | 33 (55.0%) |

*Construction and verification of the prognostic model*

The Cancer Genome Atlas-ESCC data set was classified into a training set and an internal validation set using a 1:1 ratio, and the GSE53622 served as an external validation set. First, the univariate Cox regression analysis was performed on the above crossover genes to screen the candidate genes ($P < .2$).[28] Then, the LASSO algorithm was executed on candidate genes acquired through the univariate Cox regression analysis (family = Cox). When constructing the model, the genes with coefficients of the variables retained in the model with the smallest Partial-likelihood deviance were selected; these genes were used to construct the multivariate cox model, and when constructing the multivariate cox model, the models were scored using the STEPWISE algorithm. The genes retained in the highest scoring model were selected as the key genes, and the highest scoring model was the final risk scoring model used. A stepwise approach was then performed to optimize the model and identify prognostic genes. This process resulted in the creation of a risk model of prognostic genes.

To divide samples into high- and low-risk groups, the risk score for each sample was computed using the expression levels of these prognostic genes. The risk score was computed according to the median value of risk as follows: (risk score $= \sum_1^n \text{coef}(\text{genei}) * expression(\text{genei})$). In addition, the prognostic model underwent evaluation and verified in all 3 data sets. The Kaplan-Meier (K-M) survival curve and receiver operating characteristic (ROC) curve (1-, 2-, and 3-year survival predictions) were plotted, respectively. Ultimately, based on the prognostic genes, principal component analysis (PCA) analysis was conducted based on the prognostic genes in the 3 data sets, offering insights into the relationships and patterns within the data.

*Independent prognostic analysis*

First, the univariate Cox regression analysis was implemented on the risk score and clinical features such as tumor pathologic T-M-N, stage, gender, and age. Then, the variables obtained by the univariate Cox regression analysis were used to create the multivariate Cox model. The proportional hazards (PH) hypothesis test was implemented to verify the validity of the Cox model. Furthermore, according to the above prognostic model, a nomogram for forecasting survival rates of patients with ESCC (1-, 2-, and 3 year survival rates) was created. Finally, we drew a calibration curve to verify the effectiveness of the above model.

*Differential expression analysis and enrichment analysis*

Differentially expressed genes between the 2 risk subgroups were acquired by the DESeq2 (v1.36.0) R package ($P < .05$ and $|\log_2 FC| > 2$).[25] To explore the associated biological functions and signaling pathways of the above DEGs, the GO and Kyoto Encyclopedia of Genes and Genomes (KEGG) functional enrichment analyses were performed using the clusterProfiler (v3.8.1) R software package (adjusted $P < .05$).[27]

*Genetic mutation analysis*

The mutation analysis of prognostic genes in the TCGA-ESCC data set was conducted using the maftools (v2.12.0) R package.[29] The mutual exclusion and co-occurrence of the most common top 25 mutant genes were analyzed using the CoMEt algorithm.

*Analyses of immune characteristics*

To further explore the immune infiltration environment of ESCC, the CIBERSORT algorithm was performed on the samples in the TCGA-ESCC data set. This algorithm estimates the abundance of 22 different immune cell types, allowing for a comparison of immune cell populations between the 2 risk subgroups. In addition, in the TCGA-ESCC data set, the differential immune cells between the 2 risk subgroups were computed and compared by ssGSEA algorithm and Wilcoxon test method, respectively. The risk score was computed using the expression of prognostic genes in the IMvigor210 data set. The best cut-off threshold for risk score classification was calculated using the surv-cutpoint function,

resulting in the classification of samples into high-risk and low-risk groups. Finally, we conducted a K-M survival analysis between the 2 risk subgroups to evaluate the prognostic value of the risk score in predicting patient survival.

## Drug sensitivity prediction

The $IC_{50}$ of chemical drugs for patients with ESCC was forecasted according to the cell line expression profile and gene expression profile in GDSC online database (https://www.can-cerrxgene.org/). The Oncopredict tool was used to compute the $IC_{50}$ of common chemotherapy and molecular-targeted drugs in patients with ESCC. Besides, the Wilcoxon test method was used to analyze the $IC_{50}$ of chemical drugs with remarkable differences in sensitivity between the 2 risk subgroups.

## Statistical analysis

All the analyses were implemented in the R (v4.2.0) package and the related public databases. The Wilcoxon rank-sum test was used for comparison between 2 groups. Cox and Lasso regression analysis were used to reduce the dimension of model-related risk IRRGs and construct a polygenic prognostic risk model. Kaplan-Meier survival curves are plotted and log-rank test was conducted between different subgroups. Receiver operating characteristic curves were constructed for predicting survival at 1, 2, and 3 years. A 2-sided $P < .05$ was considered statistically significant.

## Results

### Identification of IRRGs DEGs of P. gingivalis–infected ESCC

In our study, we identified 365 DEGs in the self-sequencing data set, including 217 up-regulated and 148 down-regulated genes between the *P. gingivalis*-infected group and the *P. gingivalis*-uninfected group (Figure 2A, Supplementary Table 1). Moreover, within the TCGA-ESCC data set, we found 9817 DEGs between the tumor and normal samples, of which 4989 were up-regulated and 4833 were down-regulated (Figure 2B, Supplementary Table 2). The respective expression of these DEGs was shown in heat maps (Figure 2C and D). In addition, 3074 IRRGs were gathered from the GeneCards online database according to a score threshold >5. According to the intersection of DEGs in the self-sequencing data set, DEGs in the TCGA-ESCC data set, and the set of IRRGs, 66 crossover genes were identified using a Venn map (Figure 2E). According to the enrichment analysis, crossover genes were primarily linked to biological processes like "epidermis development," "skin development," and "cytokine-mediated signaling pathway" in GO terms (Figure 2F, Supplementary Table 3).

### Construction of risk models

There were 7 candidate genes including *TNFRSF12A*, *REEP1*, *DKK1*, *FOXN1*, *ESRRB*, *EREG*, and *RELN* (Figure 3A). A

total of 6 candidate prognostic genes (*TNFRSF12A*, *DKK1*, *FOXN1*, *ESRRB*, *EREG*, and *RELN*) were identified by the LASSO algorithm (Figure 3B). According to the multivariate Cox regression analysis, 4 prognostic genes including *DKK1*, *ESRRB*, *EREG*, and *RELN* were screened out. Notably, the expressions of *DKK1*, *ESRRB*, and *EREG* negatively related to the prognosis, while *RELN* exhibited the opposite pattern (Figure 3C). A prognostic signature for patients with ESCC was constructed based on the expressions of these 4 prognostic genes and their Cox regression coefficient (β). The risk score was computed as follows: Riskscore = $(-0.33617 \times DKK1$ expression) + $(-0.57111 \times ESRRB$ expression) + $(-0.27303 \times EREG$ expression) + $(0.319031 \times RELN$ expression). The prognostic model's performance was assessed, demonstrating a C-index of 0.73, which was substantially higher than the C-index of the individual genes (Figure 3D). This indicates that the model has a strong predictive ability for patient prognosis.

### Validation of the prognostic risk model

The risk scores of high- and low-risk groups were significantly different across these 3 data sets, $(P < .05)$. Moreover, the number of deaths increased in all 3 data sets with an increased in the risk score. The expression of prognostic genes in the 3 data sets was displayed in the heat maps (Figure 4A to C). The expression of *DKK1*, *ESRRB*, and *EREG* were elevated in the low-risk group, whereas *RELN* was decreased. The accuracy of predicting 1-, 2-, and 3-year survival prognosis was evaluated using the time ROC curve and area under the curve (AUC) value. The results showed that the AUCs of the ROC curves were all exceeded 0.6 in both the training set and external validation set, indicating that the created risk model could effectively predicted the survival rates of patients with ESCC (Figure 4D to F). Next, we plotted a confusion matrix for risk grouping versus survival status, which showed an accuracy of 0.5823, a sensitivity of 0.7750, and a specificity of 0.3846 (Supplementary Figure 1). Furthermore, K-M analysis indicated that there was a remarkable difference in the prognosis of patients with ESCC between 2 risk subgroups, with the high-risk group having significantly worse outcomes than those in the low-risk group in all 3 data sets $(P < .05)$ (Figure 5A to C). Finally, there were obvious differences in the patterns of gene expression among the 2 risk subgroups in the 3 gene sets, supporting the notion that the prognostic genes could effectively distinguish between these 2 risk subgroups (Figure 5D to F).

### The nomogram for overall survival prediction

We found that risk score, pathologic N, and gender were all connected with the survival and prognosis of patients with ESCC (Figure 6A). Meanwhile, the model's overall performance was assessed, yielding a *P* value of .0165 and a C-index of 0.66 (Figure 6B), indicating a significant overall association with survival outcomes and a moderate level of predictive accuracy. The PH hypothesis test showed that neither the individual covariates
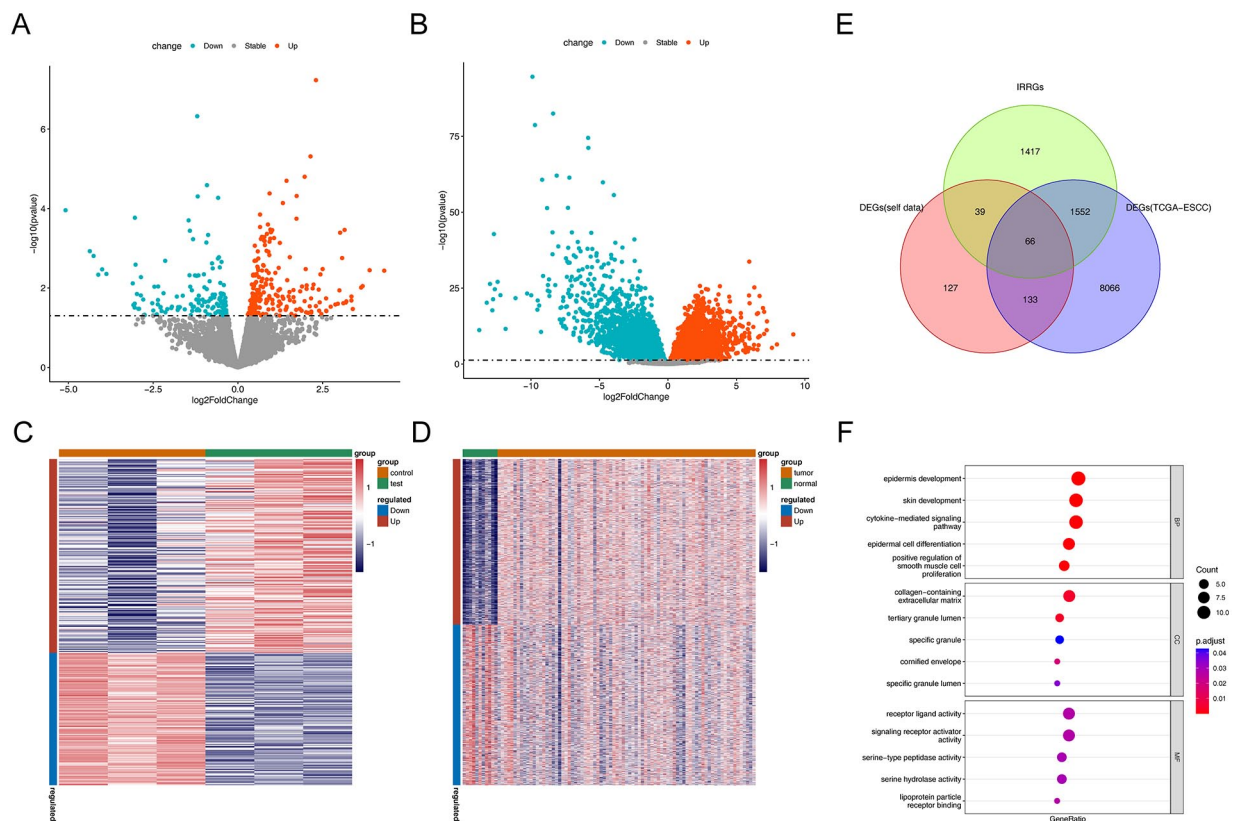
**Figure 2.** Identification of candidate IRRGs. (A) the volcano plot of DEGs between *P. gingivalis*-infected and *P. gingivalis*-uninfected ESCC cells. (B) The volcano plot of DEGs in the TCGA-ESCC data set. (C) The clustering heat map of the DEGs between *P. gingivalis*-infected and *P. gingivalis*-uninfected ESCC cells. (D) The clustering heat map of the DEGs in the TCGA-ESCC data set. (E) The Venn diagram to identify DEGs. (F) Representative results of GO analyses in TCGA.

nor the global test were statistically significant (*P* > .05). Therefore, the Cox model conformed to the PH assumption (Figure 6C). Moreover, a nomogram for survival forecasting in patients with ESCC (1, 2, and 3 years) was created based on risk score, pathologic N, and gender. The nomogram estimates the overall survival (OS) by adding up the points assigned to each parameter based on the provided scale. The risk score was found to have a substantial contribution to prognosis (Figure 6D). Finally, a calibration curve was plotted to assess the effectiveness of the nomogram. The curve indicated that the nomogram model had favorable prediction ability (Figure 6E).

*Functional enrichment analysis of DEGs in high-and low-risk groups*

There were 205 DEGs between the 2 risk subgroups (Figure 7A, Supplementary Table 4). The expression of DEGs is shown in the heat map (Figure 7B). According to the GO analysis, DEGs between the 2 risk subgroups are mainly involved in the xenobiotic metabolic process, cellular response to xenobiotic stimulus, and retinoid metabolic process in biological processes. For cellular components, DEGs were enriched in components like the integral component of the synaptic membrane, an intrinsic component of the synaptic membrane, and an integral component of the postsynaptic membrane. For molecular functions, the DEGs were linked to activities such as carboxylic

ester hydrolase activity, monocarboxylic acid binging, and glutathione transferase activity. The KEGG pathways enrichment analysis results indicated that the DEGs between the 2 risk subgroups were primarily participated in chemical carcinogenesis-receptor activation, metabolism of xenobiotics by cytochrome P450, drug metabolism-cytochrome P450, chemical carcinogenesis-DNA adducts, and drug metabolism-other enzymes (Figure 7C to F, Supplementary Table 5-6).

*Genetic mutation analysis in high- and low-risk groups*

From the TCGA-ESCC data set, the proportion of missense mutations was the highest among the mutation types, and the top 10 mutated genes were *TP53*, *TTN*, *KMT2D*, *CSMD3*, *NFE2L2*, *NOTCH1*, *MUC16*, *FLG*, *PIK3CA*, and *DNAH5* (Figure 8A). It was found that *TP53* had the highest mutation rate amongst all genes in both subgroups. In the high-risk group, mutations in *NFE2L2*, *CSMD3*, and *MUC16* were most prevalent. In contrast, in the low-risk group, *DNAH5*, *KMT2D*, and *MUC17* had a higher mutation rate (Figure 8B). Notably, *KMT2D* and *TP53* exhibited mutual exclusivity, meaning these 2 genes were less likely to co-occur in the same patient, in the low-risk group. In addition, certain genes such as *FAT3* and *TTN*, *COCH*, and *SACS*, exhibited obvious co-occurrence, suggesting that mutations in these gene pairs were
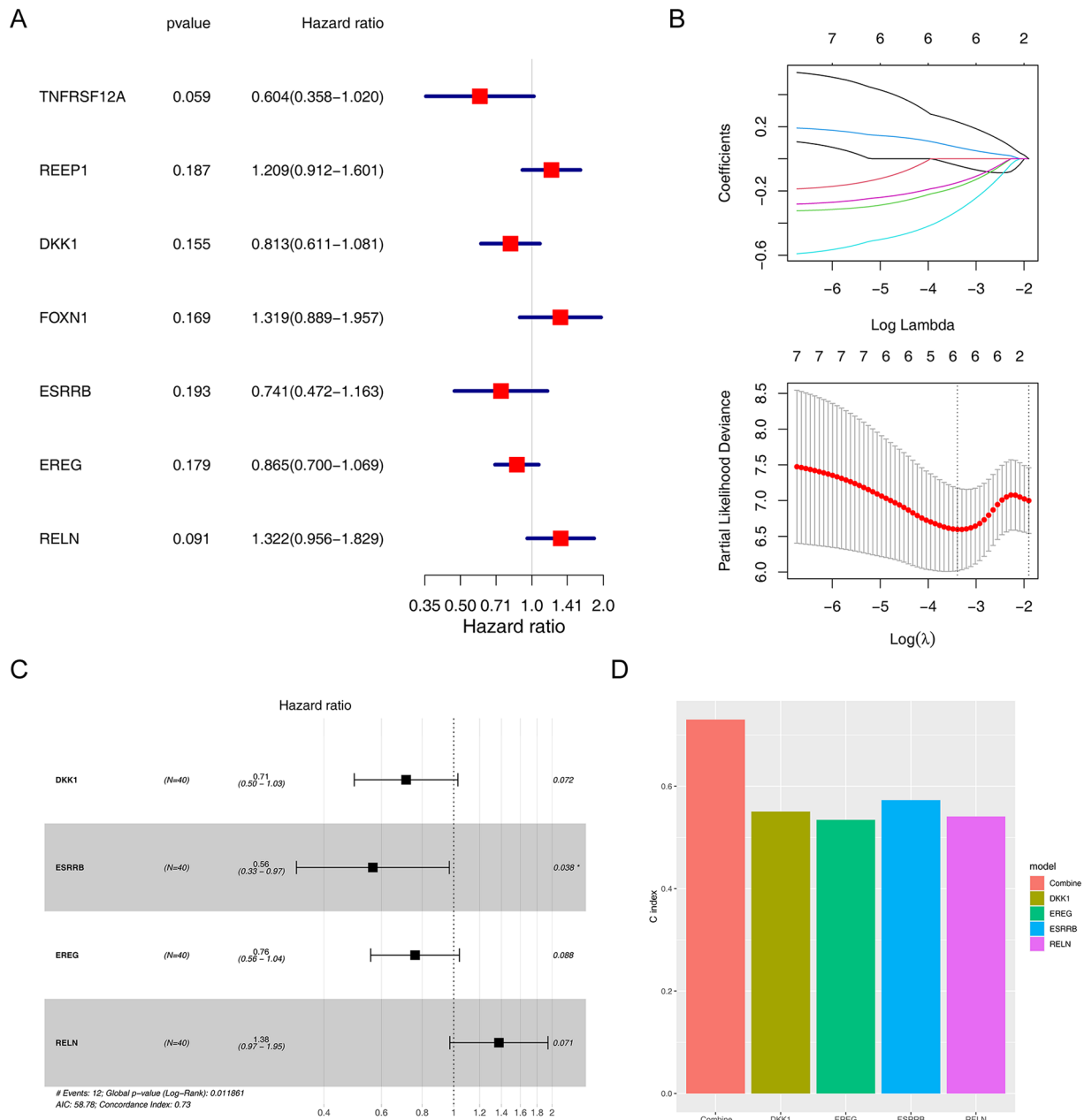
**Figure 3.** Screening of prognostic genes and construction of prognostic models. (A) The prognostic genes identified by univariate analysis in the TCGA cohort. (B) LASSO coefficient profiles and selection of the number of genes by LASSO analysis. (C) The 4 target genes identified by multivariate Cox regression analysis. (D) The C-index value of the prognostic model and prognostic gene.
*P < .05.

more likely to appear together in the same patient, in the low-risk group. Furthermore, no genes showed obvious mutual exclusion in the high-risk group, but there was an obvious co-occurrence between *MUH13* and *FLG*, as well as between *MUH13* and *ELAPOR2* (Figure 8C and D).

*Analyses of immune characteristics in high- and low-risk groups*

The abundance of immune cells in the 2 subgroups was displayed in Figure 9A. The results showed remarkable differences in 3 immune cells (activated dendritic cells [DCs], type 2 T helper cells, and neutrophils) among the 2 risk subgroups (Figure 9B). The composition of these immune cells was found to be more abundant in the low-risk group compared with the high-risk group. The IMvigor210 data set was used to analyze the relationship and predictive power of risk score for programmed death ligand 1 (PD-L1) immune efficacy. There was little difference in the number of patients with stable disease between the 2 subgroups; however, the number of patients with ESCC with partial remission and complete remission in the high-risk group was significantly higher (Figure 9 C). We also found a statistical significance in survival prognosis between the 2 subgroups, and the lower risk scores had poorer OS ($P = 0.029$) (Figure 9D).
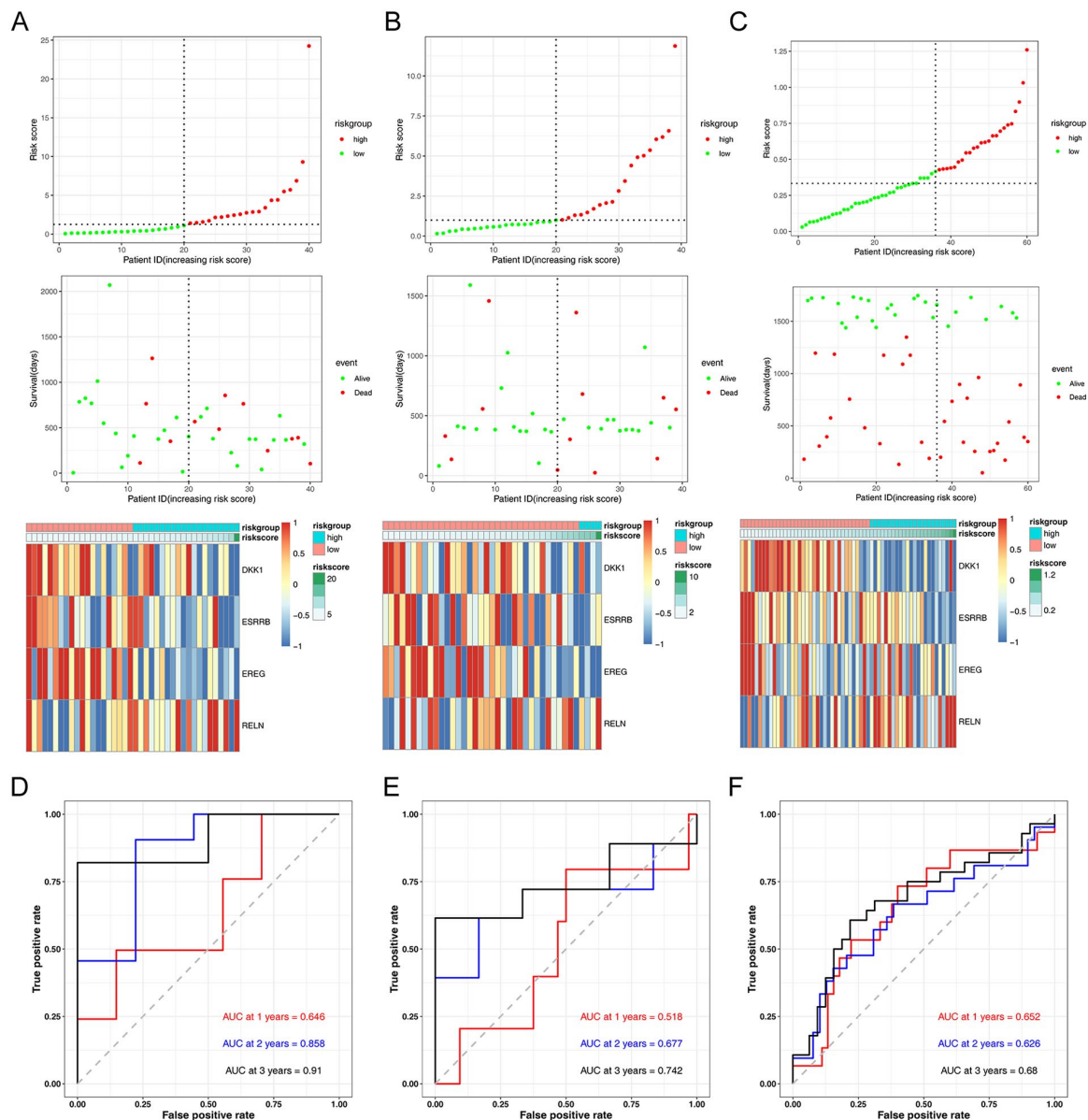
**Figure 4.** Validation and evaluation of risk models in both the TCGA and GEO cohorts. (A to C) The distribution of the risk scores (top), survival status (middle), and expression heat map of the 4 IRRGs (bottom). (D to F) The time ROC curve for OS.

## *Drug sensitivity prediction in high- and low-risk groups*

The analysis identified 41 drugs with a statistical difference in $IC_{50}$ values between the 2 risk subgroups. Notably, drugs such as sepantronium bromide, dactinomycin, and luminespib all exhibited lower $IC_{50}$ values in the low-risk group ($P < .001$) (Figure 9E). On the whole, low-risk groups were more susceptible to sepantronium bromide, dactinomycin, and luminespib which means these patients may have a more favorable response to these drugs, potentially leading to improved treatment outcomes.

## Discussion

Esophageal cancer is a malignant tumor with high mortality. With the advancement of medical technology, a variety of

treatment methods have been improved for ESCC. However, we often cannot accurately forecast the effectiveness of ESCC treatment because of lack reliable biomarkers. Numerous studies have indicated that *P. gingivalis* and inflammation response play a crucial role in the pathophysiology and malignant progression of ESCC, which is associated with patient prognosis.[5,9] However, the role of *P. gingivalis* and IRRGs as prognostic predictors for ESCC remains to be elucidated. Thus, it is particularly critical to explore accurate biomarkers for predicting prognosis of *P. gingivalis*-infected ESCC patients. In this study, we first constructed and verified a prognostic gene signature composed of *P. gingivalis* and inflammation-related DEGs, namely *DKK1*, *ESRRB*, *EREG*, and *RELN*. This signature serves as an independent risk factor to forecast the prognosis of patients with ESCC. Furthermore, we established straightforward and user-friendly
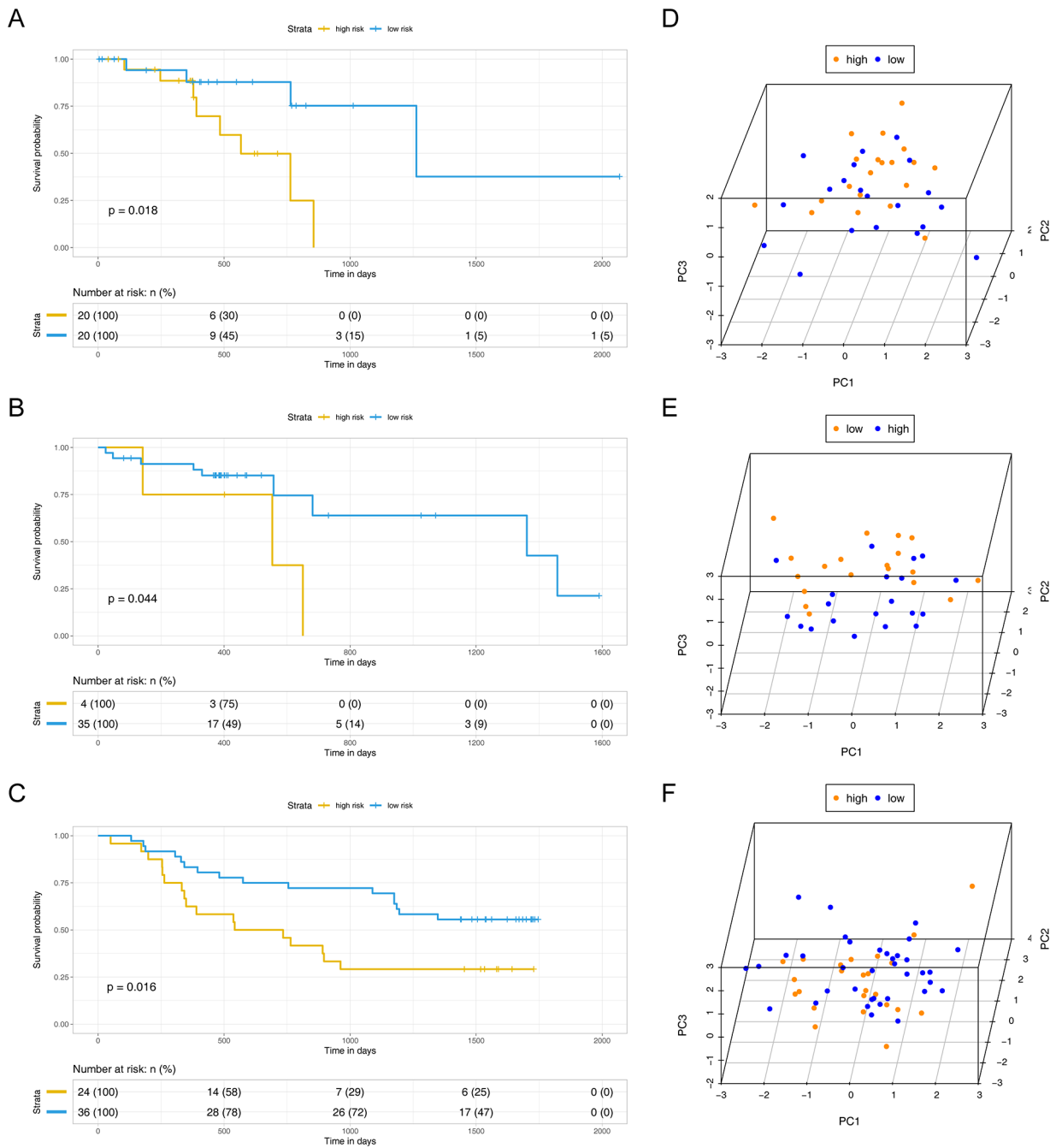
A



B



C



D



E



F



**Figure 5.** High and low risk group survival analysis and PCA validation. (A to C) Kaplan-Meier curves for OS in the high- and low-risk groups. (D to F) PCA plot in the high- and low-risk groups.

prognostic nomogram model to assist in forecasting the 1-, 2-, and 3-year OS, which may contribute to the clinical treatment of patients with ESCC. Although the prognostic model established in this study through the cell models *in vitro* is not representative of the microenvironment *in vivo*, previous studies have confirmed that *P. gingivalis* infection cells in *vitro* can affect the tumor microenvironment and promote the development of tumors.[12,13,30]

Previous research has established the roles of these 4 prognostic genes in cancer progression. *DKK1* encodes a secreted protein that is an antagonist of the Wnt/b-catenin signaling pathway, which is participate in tumor progression and is overexpressed in numerous human tumors.[31,32] *DKK1* is closely linked to prognosis and has been identified as a possible diagnostic and prognostic indicator for ESCC.[33,34] Recent research has evidenced that *DKK1* stimulates cancer cell proliferation by activating the PI3K-AKT pathway.[35] Furthermore, *DKK1* has been demonstrated to sustain the tumor stemness of EC cells through ALDH1A1/SOX2 axis.[36] *ESRRB*, a nuclear transcription factor, controls self-renewal and pluripotency of embryonic stem cells.[37] Studies have discovered that *ESRRB* is associated with tumor progression of breast and prostate cancers.[38,39] In addition, *ESRRB* accelerates the growth of carcinoma cells *in vitro* and *in vivo* by repressing the
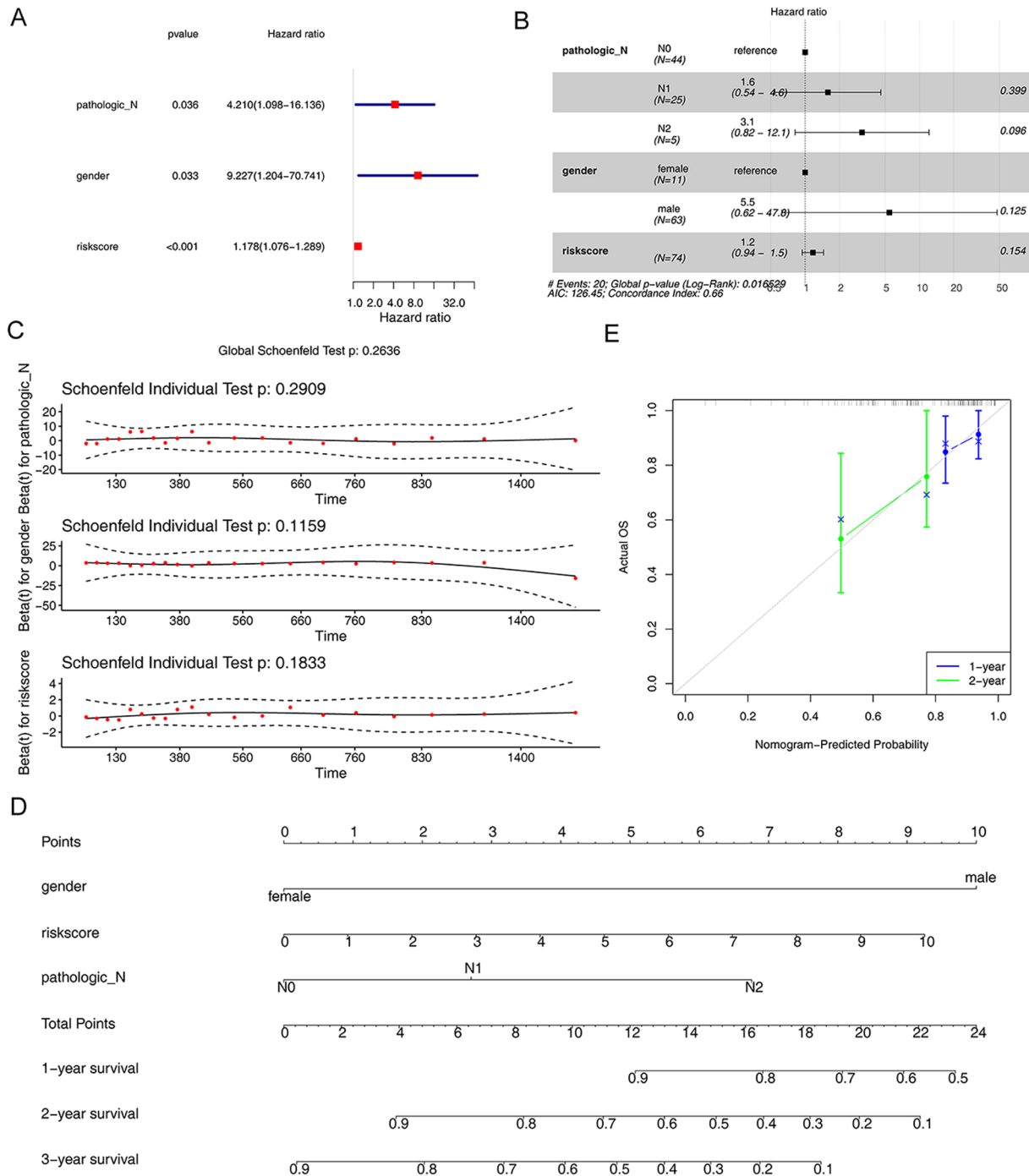
**Figure 6.** The nomogram constructed in the TCGA-ESCC cohort. (A) Forest plots for univariate cox regression analysis. (B) Forest plots of independent prognostic model. (C) PH hypothesis test. (D) The nomogram for predicting OS. (E) Calibration curves for the nomogram.

TGF-β pathway by transactivating SMAD7.[40] Our study represents the first discovery of *ESRRB* as a prognostic biomarker for ESCC, although further studies are warranted to elucidate its prognostic significance and its underlying mechanisms in patients with ESCC. *EREG*, a ligand for the estimated glomerular filtration rate (EGFR) family, contributes to processes including angiogenesis, vascular remodeling, cell proliferation, and inflammation.[41] Previous studies have noted that *EREG* is typically low or absent in most human tissues but is found to be over-expressed in various tumors.[42] *EREG* has been

involved in promoting the invasion of EC, formation of spheres, reorganization of actin, and lung metastasis by activating FAK and Src.[43] *RELN* is a well-known large extracellular matrix glycoprotein expressed primarily in brain development, where it regulates neuronal migration, adhesion, and positioning.[44] However, recent investigations have shown abnormal expression patterns of *RELN* in various cancers.[45] *RELN* is a critical negative regulator during TGF-β1-induced cell migration of Kyse-30 cells and is inhibited through the TGF-β pathway via Snail regulation at the transcriptional
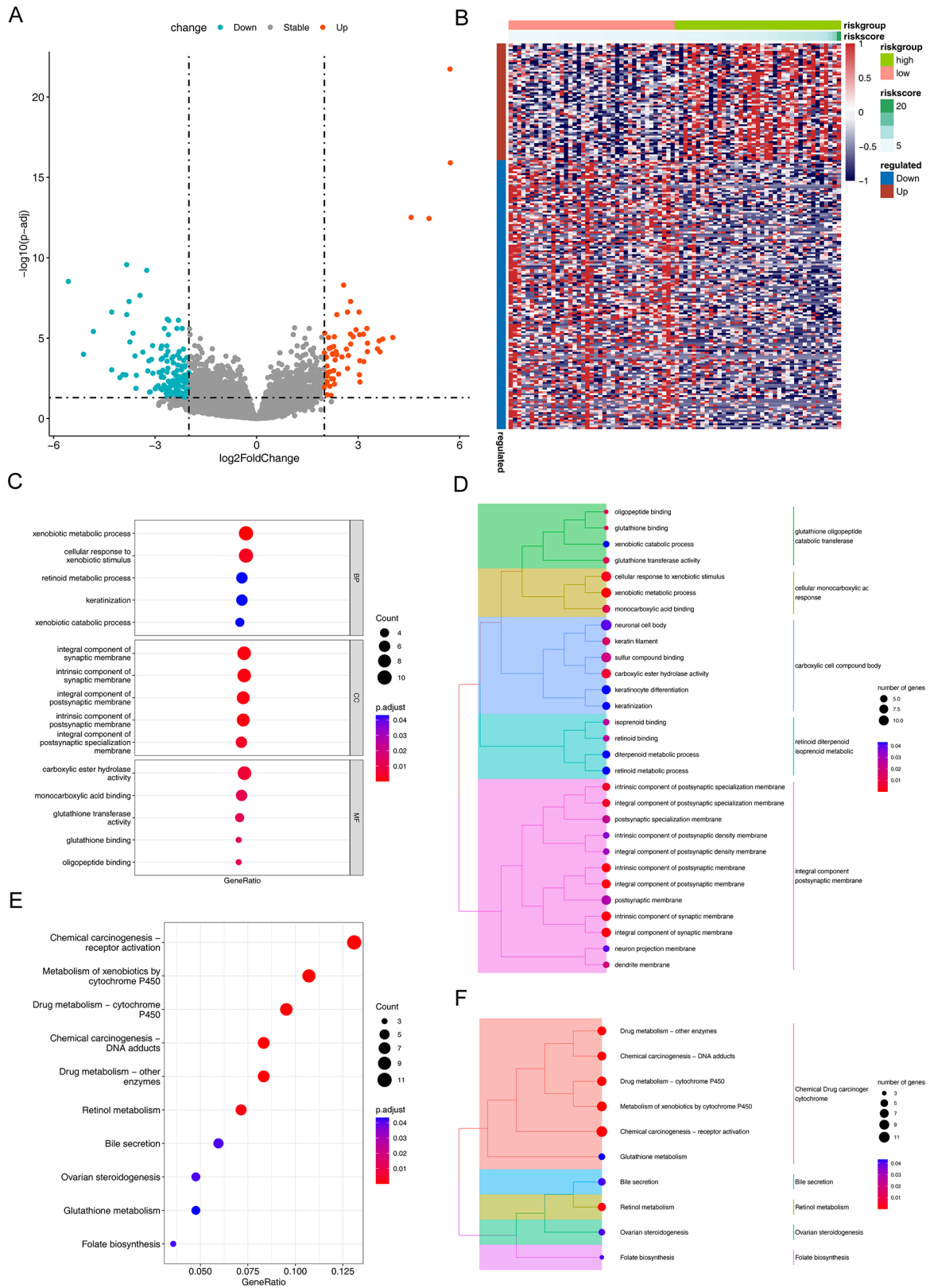
**Figure 7.** GO and KEGG analyses using the DEGs between the high- and low-risk groups. (A) Volcano plots of the DEGs. (B) The heat map of DEGs. (C and D) GO enrichment analysis based on DEGs. (E and F) KEGG enrichment analysis based on DEGs.

level.[46] Our study found high expressions of *DKK1* and *EREG* and low expressions of *ESRRB* and *RELN* in patients with ESCC, which was consistent with the above studies. Therefore, it is speculated that *DKK1*, *ESRRB*, *EREG*, and *RELN* serve as key regulatory factors in the carcinogenic process of *P. gingivalis*.
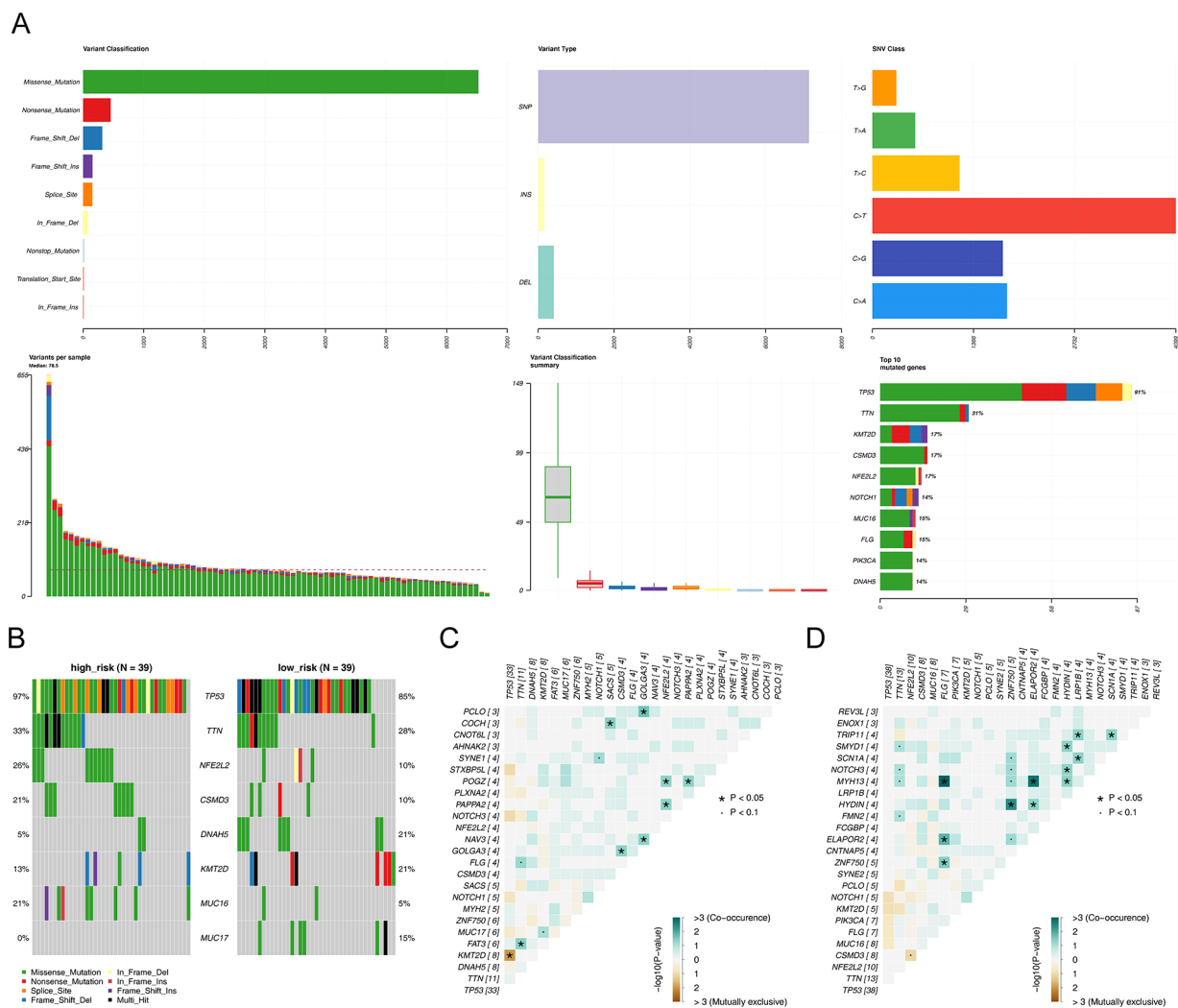
**Figure 8.** Genetic mutation in high- and low-risk groups of patients with ESCC. (A) An overview of genetic mutations. (B) The waterfall plot of genetic mutation features. (C) Co-occurrence and mutual exclusion of mutated genes in the low-risk group. (D) Co-occurrence and mutual exclusion of mutated genes in the high-risk group.

Then, we would like to further analyze the underlying mechanism of IRRGs in *P. gingivalis*-infected ESCC. The findings from KEGG and GO analyses indicated that DEGs primarily participated in processes such as the chemical carcinogenesis-receptor activation, metabolism of xenobiotics by cytochrome P450, drug metabolism-cytochrome P450, chemical carcinogenesis-DNA adducts. For instance, CYP2C9 participates in the metabolism of tumor drugs and exogenous carcinogens, which suppresses the invasion and migration of ESCC by reducing the levels of HDAC.[47] Similarly, CYP1A1 is involved in the oxidative conversion of xenobiotics, whereas its metabolic reactions may unintentionally result in the production of highly reactive compounds, which can form DNA adducts, thereby promoting mutagenesis and carcinogenesis.[48] The findings suggested that *P. gingivalis* could affect the changes in the ESCC metabolic pathway by regulating IRRGs.

Numerous pieces of evidence have demonstrated that the tumor immune microenvironment plays a crucial role in carcinogenesis. The results showed that the immune state was significantly different between the low- and high-risk patients with ESCC. Notably, immune-infiltrating cells were more abundant in the low-risk group, with heightened levels of activated DCs, type 2 T helper cells, and neutrophils. This suggests that immune regulation may be inhibited in the high-risk group, contributing to a worse prognosis in patients with ESCC. Dendritic cells are specialized antigen-presenting immune cells, which have a crucial function in the immune response against cancer.[49] Furthermore, research has indicated that increases in the number of DCs can improve immune function and extend the survival time of patients with EC.[50] Dendritic cells can kill tumor cells by stimulating the proliferation of T cells, ultimately inhibiting tumor cell proliferation and metastasis.[51] Type 2 T helper cells have an important influence on type-2 immune responses and enhance the production of antibody against extracellular tissue.[52] Research has shown the infiltration level of type 2 T helper cells is positively correlated with OS in patients with ESCC without chemotherapy after surgery, with higher infiltration levels of these cells associated with longer
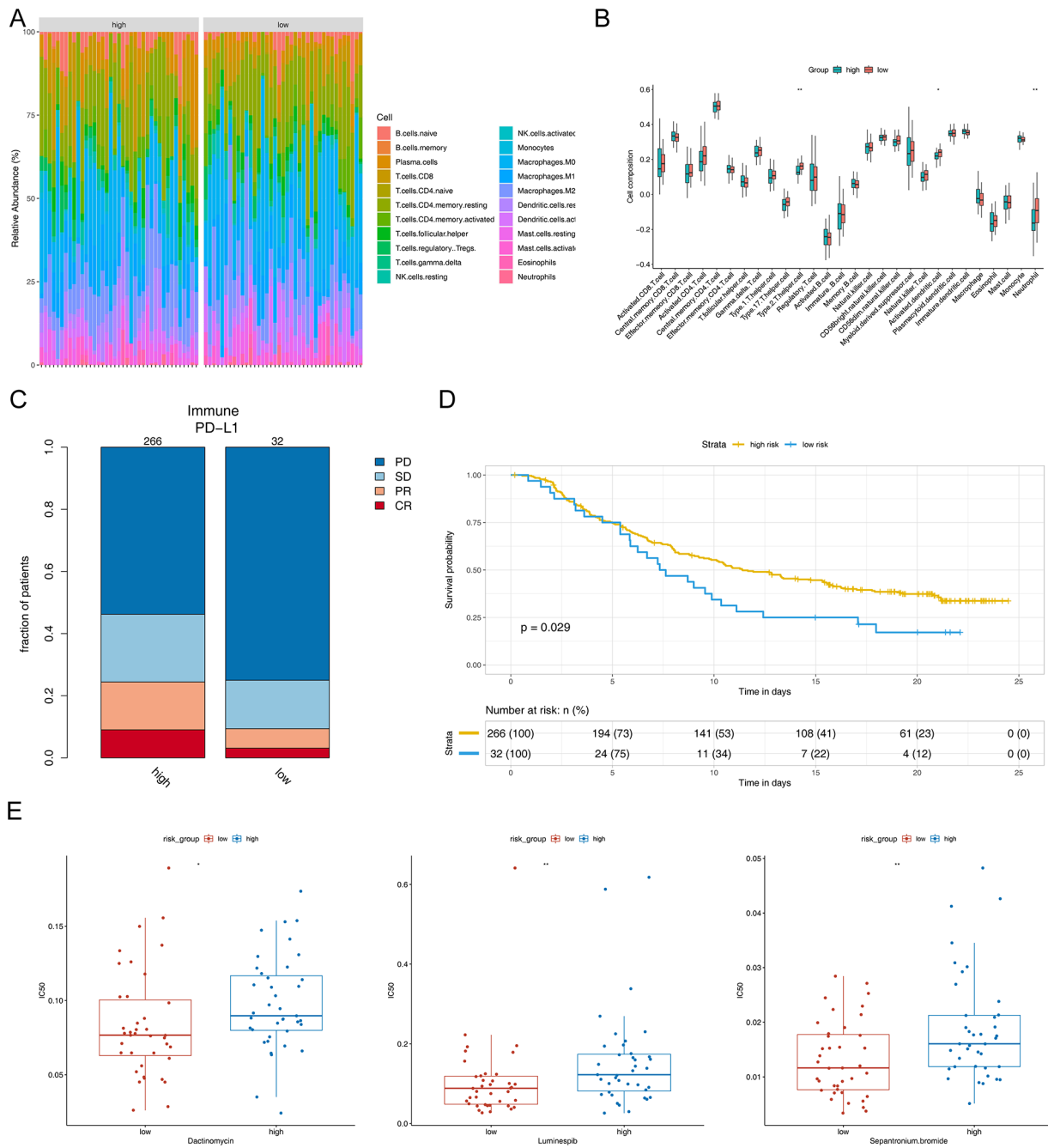
**Figure 9.** Immune characterization correlation analysis and drug susceptibility prediction. (A) Immune cell abundance map of each sample. (B) The boxplots of immune infiltration analysis. (C) Comparison of efficacy of immunotherapy between the 2 groups. (D) Kaplan-Meier curves of the OS in external validation data sets. (E) Sensitivity to dactinomycin, luminespib, and sepantronium bromide shown in the box plot.
*P < .05; **P < .01.

OS.[53] However, in the context of long-term inflammation, type 2 T helper cells have been associated with tumor promotion by provoking humoral immune responses and interfering with the recruitment and activation of cytotoxic T lymphocytes in tumor.[54] Neutrophils, often considered the first line of defense against inflammations and infections,[55] can adopt differential states of activation and differentiation in various tumor contexts. They can polarize into either an anti-cancerous (N1) type or a cancer-promoting (N2) type.[56] A recent research identified that MPO + neutrophils infiltrating the tumor were associated

with a positive prognosis for ESCC.[57] When TGF-β is not present, the N1 neutrophils secrete more immune activating cytokines and chemokines, with lower levels of arginase, and exhibit an improved capacity to eliminate cancerous cells *in vitro* and *in vivo*.[58] In summary, the immune cells above are potentially involved in the regulation of immune response in EC development and are thought to be beneficial for survival, consistent with the observations of our current study. Notably, our research identified a decrease in the proportion of type 2 T helper cells, activated DCs, and neutrophils in high-risk patients

with *P. gingivalis* infection. Therefore, it is speculated that *P. gingivalis* may weaken the antitumor immune response of the body by inhibiting the above immune cell infiltration. This could potentially be a significant factor contributing to the unfavorable prognosis of high-risk patients.

Finally, we further analyzed the drug sensitivity for ESCC according to the GDSC database. We discovered that the low-risk group was susceptible to chemotherapy drugs, for example, sepantronium bromide, dactinomycin, and luminespib. Sepantronium bromide (YM155), a survivin suppressant, has been demonstrated to enhance the radiation sensitivity of ESCC cells by suppressing radiation-induced senescence and promoting apoptosis.[59] In addition, YM155 improves radiosensitization by disrupting the G2 checkpoint and inhibiting homologous recombination repair in ESCC.[60] Luminespib, an HSP90 inhibitor, exhibits a strong antiproliferative effect for ESCC, hinting at it may become a new choice for the treatment of ESCC.[61] Therefore, the results of our study may hold promise in guiding decisions related to immunotherapy and chemotherapy, with the potential to inform clinical treatment strategies for patients with ESCC.

Our research has some limitations. First, for data selection bias, matching and sensitivity analyses can be further used in the future to reduce possible selection bias in the database. Then by comparing the results with external validation, the impact of selection bias on the findings can then be assessed and the generalizability, and reliability of the results can be improved. Second, our study was retrospectively analyzed, and the outcomes were only verified using the TGCA and GEO data sets, which requires more prospective studies and a large cohort of clinical tissue samples to validate the identified signatures and assess their relevance to immunity, prognosis, and resistance. In the future, our team keep on to explore this field. Finally, though *P. gingivalis* is related to the occurrence and development of ESCC, and the infection rate of *P. gingivalis* is about 60% due to individual differences and the influence of tumor microenvironment on micro-organisms. Hence, we established the prognostic model only for ESCC patients with *P. gingivalis* infection.

Although there are some limitations in our study, this does not affect the value of this study. First, the effect of IRRGs on the prognosis of *P. gingivalis*-infected ESCC patients has never been reported. Second, the predictive model is beneficial for more accurately predicting the prognosis of *P. gingivalis*-infected ESCC patients and improving the survival rate of patients. In the future, we can conduct more detailed microbiome analysis for patients with different subtypes of ESCC, as well as more in-depth studies combined with clinical data to verify the association between oral microbes and ESCC. In brief, our study not only reveals their role in ESCC but also lays the foundation for the early diagnosis and precision medicine of tumor.

## Conclusions

In conclusion, we successfully developed a new predictive model for patients with ESCC, leveraging 4 IRGGs with

prognostic significance. Moreover, our research also assessed the potential of the risk model to predict infiltration of immune cells and sensitivity to chemotherapy, thereby enhancing its clinical utility and providing potential biomarkers for clinical therapeutic strategies.

## Author Contributions
JK wrote and revised the article. LX conceived and revised the article. JK and MQ contributed to the experimental studies. YL, JW, and WS revised the article and edited part of the manuscript. All authors read and approved the final manuscript.

## Availability of Data and Materials
The data sets involved in the study were all obtained from the TCGA database (https://www.cancer.gov/ccg/) and the GEO database (https://www.ncbi.nlm.nih.gov/geo/). All fastq raw sequence read data have been uploaded to the NCBI Sequence Read Archive (SRA) under accession number PRJNA1047328.

## Consent for Publication
Not applicable

## Ethics Approval and Consent to Participate
Not applicable

## ORCID iD
Jinyu Kong   https://orcid.org/0000-0002-7797-7878

## Supplemental Material
Supplemental material for this article is available online.

## REFERENCES

1. Sung H, Ferlay J, Siegel RL, et al. Global cancer statistics 2020: GLOBOCAN estimates of incidence and mortality worldwide for 36 cancers in 185 countries. *CA Cancer J Clin*. 2021;71:209-249. doi:10.3322/caac.21660
2. Abnet CC, Arnold M, Wei WQ. Epidemiology of esophageal squamous cell carcinoma. *Gastroenterology*. 2018;154:360-373. doi:10.1053/j.gastro.2017.08.023
3. Cao W, Chen HD, Yu YW, Li N, Chen WQ. Changing profiles of cancer burden worldwide and in China: a secondary analysis of the global cancer statistics 2020. *Chin Med J (Engl)*. 2021;134:783-791. doi:10.1097/CM9.0000000000001474
4. Allemani C, Matsuda T, Di Carlo V, et al. Global surveillance of trends in cancer survival 2000-14 (CONCORD-3): analysis of individual records for 37 513 025 patients diagnosed with one of 18 cancers from 322 population-based registries in 71 countries. *Lancet*. 2018;391:1023-1075. doi:10.1016/S0140-6736(17)33326-3
5. Sharma T, Gupta A, Chauhan R, et al. Cross-talk between the microbiome and chronic inflammation in esophageal cancer: potential driver of oncogenesis. *Cancer Metastasis Rev*. 2022;41:281-299. doi:10.1007/s10555-022-10026-6
6. Hussain SP, Harris CC. Inflammation and cancer: an ancient link with novel potentials. *Int J Cancer*. 2007;121:2373-2380. doi:10.1002/ijc.23173
7. Zhang Z, Liu D, Liu S, Zhang S, Pan Y. The role of *Porphyromonas gingivalis* outer membrane vesicles in periodontal disease and related systemic diseases. *Front Cell Infect Microbiol*. 2021;10:585917. doi:10.3389/fcimb.2020.585917
8. Lamont RJ, Fitzsimonds ZR, Wang H, Gao S. Role of *Porphyromonas gingivalis* in oral and orodigestive squamous cell carcinoma. *Periodontol 2000*. 2022;89:154-165. doi:10.1111/prd.12425
9. Gao S, Li S, Ma Z, et al. Presence of *Porphyromonas gingivalis* in esophagus and its association with the clinicopathological characteristics and survival in patients with esophageal cancer. *Infect Agent Cancer*. 2016;11:3. doi:10.1186/s13027-016-0049-x

10. Gao SG, Yang JQ, Ma ZK, et al. Preoperative serum immunoglobulin G and A antibodies to *Porphyromonas gingivalis* are potential serum biomarkers for the diagnosis and prognosis of esophageal squamous cell carcinoma. *BMC Cancer.* 2018;18:17. doi:10.1186/s12885-017-3905-1

11. Gao SG, Qi ZP, Qi YJ, et al. *Porphyromonas gingivalis* predicts local recurrence after endoscopic submucosal dissection of early esophageal squamous cell carcinoma or precancerous lesion. *BMC Cancer.* 2023;23:43. doi:10.1186/s12885-022-10469-8

12. Gao S, Liu Y, Duan X, et al. *Porphyromonas gingivalis* infection exacerbates oesophageal cancer and promotes resistance to neoadjuvant chemotherapy. *Br J Cancer.* 2021;125:433-444. doi:10.1038/s41416-021-01419-5

13. Liu Y, Zhou F, Yang H, et al. *Porphyromonas gingivalis* promotes malignancy and chemo-resistance via GSK3β-mediated mitochondrial oxidative phosphorylation in human esophageal squamous cell carcinoma. *Transl Oncol.* 2023;32:101656. doi:10.1016/j.tranon.2023.101656

14. Read SA, Douglas MW. Virus induced inflammation and cancer development. *Cancer Lett.* 2014;345:174-181. doi:10.1016/j.canlet.2013.07.030

15. Oh JK, Weiderpass E. Infection and cancer: global distribution and burden of diseases. *Ann Glob Health.* 2014;80:384-392. doi:10.1016/j.aogh.2014.09.013

16. Wang F, He W, Fanghui P, Wang L, Fan Q. NF-κBP65 promotes invasion and metastasis of oesophageal squamous cell cancer by regulating matrix metalloproteinase-9 and epithelial-to-mesenchymal transition. *Cell Biol Int.* 2013;37:780-788. doi:10.1002/cbin.10089

17. Chen M, Ye X, Wang R, Poon K. Research progress of cancer stem cells and IL-6/STAT3 signaling pathway in esophageal adenocarcinoma. *Transl Cancer Res.* 2020;9:363-371. doi:10.21037/tcr.2019.11.12

18. Hirano T. IL-6 in inflammation, autoimmunity and cancer. *Int Immunol.* 2021;33:127-148. doi:10.1093/intimm/dxaa078

19. Nienhüser H, Wirsik N, Schmidt T. Esophageal tumor microenvironment. *Adv Exp Med Biol.* 2020;1296:103-116. doi:10.1007/978-3-030-59038-3_6

20. Kong J, Liu Y, Qian M, Xing L, Gao S. The relationship between *Porphyromonas gingivalis* and oesophageal squamous cell carcinoma: a literature review. *Epidemiol Infect.* 2023;151:e69. doi:10.1017/S0950268823000298

21. Tan Q, Ma X, Yang B, et al. Periodontitis pathogen *Porphyromonas gingivalis* promotes pancreatic tumorigenesis via neutrophil elastase from tumor-associated neutrophils. *Gut Microbes.* 2022;14:2073785. doi:10.1080/19490976.2022.2073785

22. Sun SY, Chen PP, Meng LX, et al. High preoperative plasma fibrinogen and serum albumin score is associated with poor survival in operable esophageal squamous cell carcinoma. *Dis Esophagus.* 2019;32:1-9. doi:10.1093/dote/doy057

23. Yodying H, Matsuda A, Miyashita M, et al. Prognostic significance of neutrophil-to-lymphocyte ratio and platelet-to-lymphocyte ratio in oncologic outcomes of esophageal cancer: a systematic review and meta-analysis. *Ann Surg Oncol.* 2016;23:646-654. doi:10.1245/s10434-015-4869-5

24. He H, Zhang P, Li F, Zeng C, Liu D, Wu K. Predicting the prognosis of esophageal cancer based on extensive analysis of new inflammatory response-related signature. *J Biochem Mol Toxicol.* 2023;37:e23291. doi:10.1002/jbt.23291

25. Love MI, Huber W, Anders S. Moderated estimation of fold change and dispersion for RNA-seq data with DESeq2. *Genome Biol.* 2014;15:550. doi:10.1186/s13059-014-0550-8

26. Ito K, Murphy D. Application of ggplot2 to pharmacometric graphics. *CPT Pharmacometrics Syst Pharmacol.* 2013;2:e79. doi:10.1038/psp.2013.56

27. Wu T, Hu E, Xu S, et al. ClusterProfiler 4.0: a universal enrichment tool for interpreting omics data. *Innovation (Camb).* 2021;2:100141. doi:10.1016/j.xinn.2021.100141

28. Kang SJ, Cho YR, Park GM, et al. Predictors for functionally significant in-stent restenosis: an integrated analysis using coronary angiography, IVUS, and myocardial perfusion imaging. *JACC Cardiovasc Imaging.* 2013;6:1183-1190. doi:10.1016/j.jcmg.2013.09.006

29. Mayakonda A, Lin DC, Assenov Y, Plass C, Koeffler HP. Maftools: efficient and comprehensive analysis of somatic variants in cancer. *Genome Res.* 2018;28:1747-1756. doi:10.1101/gr.239244.118

30. Yuan X, Liu Y, Li G, et al. Blockade of immune-checkpoint B7-H4 and lysine demethylase 5B in esophageal squamous cell carcinoma confers protective immunity against *P. gingivalis* infection. *Cancer Immunol Res.* 2019;7:1440-1456. doi:10.1158/2326-6066

31. Kagey MH, He X. Rationale for targeting the Wnt signalling modulator Dickkopf-1 for oncology. *Br J Pharmacol.* 2017;174:4637-4650. doi:10.1111/bph.13894

32. Chu HY, Chen Z, Wang L, et al. Dickkopf-1: a promising target for cancer immunotherapy. *Front Immunol.* 2021;12:658097. doi:10.3389/fimmu.2021.658097

33. Begenik H, Kemik AS, Emre H, et al. The association between serum Dickkopf-1 levels and esophageal squamous cell carcinoma. *Hum Exp Toxicol.* 2014;33:785-788. doi:10.1177/0960327113510537

34. Makino T, Yamasaki M, Takemasa I, et al. Dickkopf-1 expression as a marker for predicting clinical outcome in esophageal squamous cell carcinoma. *Ann Surg Oncol.* 2009;16:2058-2064. doi:10.1245/s10434-009-0476-7

35. Kimura H, Fumoto K, Shojima K, et al. CKAP4 is a Dickkopf1 receptor and is involved in tumor progression. *J Clin Invest.* 2016;126:2689-2705. doi:10.1172/JCI84658

36. Lu Z, Zhou C, Hu J, Xiong L, Cong Z, Shen Y. DKK1 maintained cancer stem-like properties of esophageal carcinoma cells via ALDH1A1/SOX2 axis. *Int J Clin Exp Pathol.* 2017;10:9489-9495.

37. Adachi K, Kopp W, Wu G, et al. Esrrb unlocks silenced enhancers for reprogramming to naive pluripotency. *Cell Stem Cell.* 2018;23:266-275.e6. doi:10.1016/j.stem.2018.05.020

38. Naik SK, Lam EW, Parija M, et al. NEDDylation negatively regulates ERRβ expression to promote breast cancer tumorigenesis and progression. *Cell Death Dis.* 2020;11:703. doi:10.1038/s41419-020-02838-7

39. Yu S, Wong YC, Wang XH, et al. Orphan nuclear receptor estrogen-related receptor-beta suppresses in vitro and in vivo growth of prostate cancer cells via p21(WAF1/CIP1) induction and as a potential therapeutic target in prostate cancer. *Oncogene.* 2008;27:3313-3328. doi:10.1038/sj.onc.1210986

40. Li QS, Zheng PS. ESRRB inhibits the TGF-β signaling pathway to drive cell proliferation in cervical cancer. *Cancer Res.* 2023;83:3095-3114. doi:10.1158/0008-5472.CAN-23-0067

41. Riese DJ 2nd, Cullum RL. Epiregulin: roles in normal physiology and cancer. *Semin Cell Dev Biol.* 2014;28:49-56. doi:10.1016/j.semcdb

42. Cheng WL, Feng PH, Lee KY, et al. The role of EREG/EGFR pathway in tumor progression. *Int J Mol Sci.* 2021;22:12828. doi:10.3390/ijms222312828

43. Sun L, Pan J, Yu L, et al. Tumor endothelial cells promote metastasis and cancer stem cell-like phenotype through elevated Epiregulin in esophageal cancer. *Am J Cancer Res.* 2016;6:2277-2288.

44. Tissir F, Goffinet AM. Reelin and brain development. *Nat Rev Neurosci.* 2003;4:496-505. doi:10.1038/nrn1113

45. Li Z, Wang X, Yang Y, et al. Identification and validation of RELN mutation as a response indicator for immune checkpoint inhibitor therapy in melanoma and non-small cell lung cancer. *Cells.* 2022;11:3841. doi:10.3390/cells11233841

46. Yuan Y, Chen H, Ma G, Cao X, Liu Z. Reelin is involved in transforming growth factor-β1-induced cell migration in esophageal carcinoma cells. *PLoS ONE.* 2012;7:e31802. doi:10.1371/journal.pone.0031802

47. Jiang Z, Zheng X, Wang W, et al. CYP2C9 inhibits the invasion and migration of esophageal squamous cell carcinoma via downregulation of HDAC. *Mol Cell Biochem.* 2021;476:2011-2020. doi:10.1007/s11010-021-04050-3

48. Whitlock JP Jr. Induction of cytochrome P4501A1. *Annu Rev Pharmacol Toxicol.* 1999;39:103-125. doi:10.1146/annurev.pharmtox.39.1.103

49. Yang W, Yu J. Immunologic function of dendritic cells in esophageal cancer. *Dig Dis Sci.* 2008;53:1739-1746. doi:10.1007/s10620-007-0095-8

50. Liu Y, Mu Y, Zhang A, et al. Cytokine-induced killer cells/dendritic cells and cytokine-induced killer cells immunotherapy for the treatment of esophageal cancer in China: a meta-analysis. *Onco Targets Ther.* 2017;10:1897-1908. doi:10.2147/OTT.S132507

51. Correale P, Micheli L, Vecchio MT, et al. A parathyroid-hormone-related-protein (PTH-rP)-specific cytotoxic T cell response induced by in vitro stimulation of tumour-infiltrating lymphocytes derived from prostate cancer metastases, with epitope peptide-loaded autologous dendritic cells and low-dose IL-2. *Br J Cancer.* 2001;85:1722-1730. doi:10.1054/bjoc.2001.2136

52. Lorvik KB, Hammarström C, Fauskanger M, et al. Adoptive transfer of tumor-specific Th2 cells eradicates tumors by triggering an in situ inflammatory immune response. *Cancer Res.* 2016;76:6864-6876. doi:10.1158/0008-5472

53. Peng L, He W, Ye F, et al. Identification of tumor-infiltrating lymphocyte subpopulations correlated with patient prognosis in esophageal squamous cell carcinoma. *J Int Med Res.* 2021;49:3000605211016206. doi:10.1177/03000605211016206

54. Johansson M, Denardo DG, Coussens LM. Polarized immune responses differentially regulate cancer development. *Immunol Rev.* 2008;222:145-154. doi:10.1111/j.1600-065X.2008.00600.x

55. Matsumoto Y, Mabuchi S, Kozasa K, et al. The significance of tumor-associated neutrophil density in uterine cervical cancer treated with definitive radiotherapy. *Gynecol Oncol.* 2017;145:469-475. doi:10.1016/j.ygyno.2017.02.009

56. Sagiv JY, Michaeli J, Assi S, et al. Phenotypic diversity and plasticity in circulating neutrophil subpopulations in cancer. *Cell Rep.* 2015;10:562-573. doi:10.1016/j.celrep.2014.12.039

57. Chen CL, Wang Y, Huang CY, et al. IL-17 induces antitumor immunity by promoting beneficial neutrophil recruitment and activation in esophageal squamous cell carcinoma. *Oncoimmunology.* 2017;7:e1373234. doi:10.1080/2162402X.2017.1373234

58. Fridlender ZG, Sun J, Kim S, et al. Polarization of tumor-associated neutrophil phenotype by TGF-beta: "N1" versus "N2" TAN. *Cancer Cell.* 2009;16:183-194. doi:10.1016/j.ccr.2009.06.017

59. Liu X, Zhao Y, Zhang W, et al. Inhibition of survivin enhances radiosensitivity of esophageal cancer cells by switching radiation-induced senescence to apoptosis. *Onco Targets Ther.* 2018;11:3087-3100. doi:10.2147/OTT.S166798

60. Qin Q, Cheng H, Lu J, et al. Small-molecule survivin inhibitor YM155 enhances radiosensitization in esophageal squamous cell carcinoma by the abrogation of G2 checkpoint and suppression of homologous recombination repair. *J Hematol Oncol.* 2014;7:62. doi:10.1186/s13045-014-0062-8

61. Bao XH, Takaoka M, Hao HF, et al. Antiproliferative effect of the HSP90 inhibitor NVP-AUY922 is determined by the expression of PTEN in esophageal cancer. *Oncol Rep.* 2013;29:45-50. doi:10.3892/or.2012.2074